by the addition of galactose to 2%. An attenuated *GAL1* promoter was used to express *myc18-CDC20* in the W303 control to achieve levels close to that of the *sug1-25* mutant, which is defective in *GAL1* induction. Cells were left to grow for 1.5 h at 36 °C, then harvested. Cells were lysed with glass beads in 25 mM Tris-HCl pH 8.0, 2 mM EDTA, 1 μg ml^{-1} leupeptin, 1 μg ml^{-1} pepstatin, 2 μg ml^{-1} aprotinin, 2 mM phenylmethylsulphonyl fluoride. Protein concentrations in soluble lysates were measured with Lowry assays against a standard curve of BSA. Protein samples (100 μg) were resolved on a Tris-glycine SDS 8% polyacrylamide gel, transferred to poly(vinylidene difluoride) membrane, probed with 9E10 anti-Myc primary antibody and horseradish-peroxidase-conjugated goat anti-mouse secondary antibody.

ChIP experiments

ChIP experiments were performed essentially as described in ref. 23 and references therein. For additional details, see Supplementary Information.

Received 10 March; accepted 6 May 2003; doi:10.1038/nature01720.

1. Endicott, J. A. & Nurse, P. The cell cycle and suc1: From structure to function? *Structure* **3,** 321–325 (1995).
2. Pines, J. Cell cycle: Reaching for a role for the Cks proteins. *Curr. Biol.* **6,** 1399–1402 (1996).
3. Tang, Y. & Reed, S. I. The cdk-associated protein Cks1 functions both in G1 and G2 in *Saccharomyces cerevisiae*. *Genes Dev.* **7,** 822–832 (1993).
4. Kaiser, P. *et al.* Cyclin-dependent kinase and Cks/Suc1 interact with the proteasome in yeast to control proteolysis of M-phase targets. *Genes Dev.* **13,** 1190–1202 (1999).
5. Ghiara, J. B. *et al.* A cyclin B homolog in *S. cerevisiae*: Chronic activation of the Cdc28 protein kinase by cyclin prevents exit from mitosis. *Cell* **65,** 163–174 (1991).
6. Amon, A., Tyers, M., Futcher, B. & Nasmyth, K. Mechanisms that help the yeast cell cycle clock tick: G2 cyclins transcriptionally activate G2 cyclins and repress G1 cyclins. *Cell* **74,** 993–1007 (1993).
7. Nasmyth, K. Control of the yeast cell cycle by the cdc28 protein kinase. *Curr. Opin. Cell Biol.* **5,** 166–179 (1993).
8. Visintin, R., Prinz, S. & Amon, A. Cdc20 and cdh1: A family of substrate-specific activators of APC-dependent proteolysis. *Science* **278,** 460–463 (1997).
9. Lim, H. H., Goh, P.-Y. & Surana, U. Cdc20 is essential for the cyclosome-mediated proteolysis of both Pds1 and clb2 during M phase in budding yeast. *Curr. Biol.* **8,** 231–234 (1998).
10. Jensen, S., Segal, M., Clarke, D. J. & Reed, S. I. A novel role of the budding yeast separin Esp1 in anaphase spindle elongation: evidence that proper spindle association of Esp1 is regulated by Pds1. *J. Cell Biol.* **152,** 27–40 (2001).
11. Spellman, P. T. *et al.* Comprehensive identification of cell cycle-regulated genes of the yeast *Saccharomyces cerevisiae* by microarray hybridization. *Mol. Biol. Cell* **9,** 3273–3297 (1998).
12. Maher, M., Cong, F., Kindelberger, D., Nasmyth, K. & Dalton, S. Cell cycle-regulated transcription of the CLB2 gene is dependent on Mcm1 and a ternary complex factor. *Mol. Cell. Biol.* **15,** 3129–3137 (1995).
13. Pic, A. *et al.* The forkhead protein Fkh2 is a component of the yeast cell cycle transcription factor SFF. *EMBO J.* **19** 14, 3750–3761 (2000).
14. Koranda, M., Schleiffer, A., Endler, L. & Ammerer, G. Forkhead-like transcription factors recruit Ndd1 to the chromatin of G2/M-specific promoters. *Nature* **406,** 94–98 (2000).
15. Zhu, G. *et al.* Two yeast forkhead genes regulate the cell cycle and pseudohyphal growth. *Nature* **406,** 90–94 (2000).
16. Bourne, Y. *et al.* Crystal structure and mutational analysis of the human cdk2 kinase complex with cell cycle-regulatory protein CksHs1. *Cell* **84,** 863–874 (1996).
17. Ferdous, A., Gonzalez, F., Sun, L., Kodadek, T. & Johnston, S. A. The 19S regulatory particle of the proteasome is required for efficient transcription elongation by RNA polymerase. *Mol. Cell* **7,** 981–991 (2001).
18. Gonzalez, F., Delahodde, A., Kodadek, T. & Johnston, S. A. Recruitment of a 19S proteasome subcomplex to an activated promoter. *Science* **296,** 548–550 (2002).
19. Hilt, W., Enenkel, C., Gruhler, A., Singer, T. & Wolf, D. H. The PRE4 gene codes for a subunit of the yeast proteasome necessary for peptidylglutamyl-peptide-hydrolyzing activity. Mutations link proteasome and stress- and ubiquitin-dependent proteolysis. *J. Biol. Chem.* **268,** 3479–3486 (1993).
20. Guthrie, C., Fink, G. R. *Guide to Yeast Genetics and Molecular Biology* **194** (Academic, San Diego, California, 1991).
21. Reed, S. I., Hadwiger, J. A. & Lorincz, A. Protein kinase activity associated with the product of the yeast cell division cycle gene CDC28. *Proc. Natl Acad. Sci. USA* **82,** 4055–4059 (1985).
22. Collart, M. A. & Oliviero, S. in *Current Protocols in Molecular Biology* Vol. 2, 13.12 (Current Protocols, Wiley and Sons, New York, 1993).
23. Kaiser, P., Flick, K., Wittenberg, C. & Reed, S. I. Regulation of transcription by ubiquitination without proteolysis: Cdc34/SCFMet30-mediated inactivation of the transcription factor Met4. *Cell* **102,** 303–314 (2000).

Supplementary Information accompanies the paper on **www.nature.com/nature**.

Acknowledgements We thank S. A. Johnston for the *sug1-25* strain, M. Koranda and G. Ammerer for the tagged Mcm1 and Ndd1 strains, K. Nasymth for the *myc18-CDC20* allele, D. Wolff for the *pre1* and *pre4* strains used to construct the double mutant in our strain background, and K. Flick and S. Haase for discussions and technical advice about northern blotting experiments and ChIP assays. This work was supported by a grant from the NIH to S.I.R. M.C.M. acknowledges fellowship support from the International Agency for Research on Cancer and the Swiss National Science Foundation, and P.K. acknowledges fellowship support from the Austrian Science Foundation.

Competing interests statement The authors declare that they have no competing financial interests.

Correspondence and requests for materials should be addressed to S.I.R. (sreed@scripps.edu).

POT1 as a terminal transducer of TRF1 telomere length control

Diego Loayza & Titia de Lange

Laboratory for Cell Biology and Genetics, The Rockefeller University, 1230 York Avenue, New York, New York 10021, USA

Human telomere maintenance is essential for the protection of chromosome ends, and changes in telomere length have been implicated in ageing and cancer[1–4]. Human telomere length is regulated by the TTAGGG-repeat-binding protein TRF1 and its interacting partners tankyrase 1, TIN2 and PINX1 (refs 5–9). As the TRF1 complex binds to the duplex DNA of the telomere, it is unclear how it can affect telomerase, which acts on the single-stranded 3′ telomeric overhang. Here we show that the TRF1 complex interacts with a single-stranded telomeric DNA-binding protein—protection of telomeres 1 (POT1)—and that human POT1 controls telomerase-mediated telomere elongation. The presence of POT1 on telomeres was diminished when the amount of single-stranded DNA was reduced. Furthermore, POT1 binding was regulated by the TRF1 complex in response to telomere length. A mutant form of POT1 lacking the DNA-binding domain abrogated TRF1-mediated control of telomere length, and induced rapid and extensive telomere elongation. We propose that the interaction between the TRF1 complex and POT1 affects the loading of POT1 on the single-stranded telomeric DNA, thus transmitting information about telomere length to the telomere terminus, where telomerase is regulated.

Telomeric DNA can be maintained by telomerase, which uses the 3′ end of the telomeric overhang as a substrate. In germline and tumour cells, the length of the duplex telomeric repeat array is kept within a narrow range by telomere length homeostasis. Extensive evidence indicates that the length of human telomeres is evaluated at each individual chromosome end based on the amount of TRF1 complex bound along the length of the telomere[5–8,10–14]. An analogous *cis*-acting 'protein counting' mechanism of the duplex telomere-binding protein Rap1 (ref. 15) has been proposed for the control of telomere length in budding yeast. However, it is not clear how regulatory proteins engaged on the duplex part of the telomere affect telomerase at the 3′ end of the telomeric overhang. In yeast, the 3′ overhang is bound by Cdc13, which recruits and regulates telomerase[16], but there is no known connection between Cdc13 and Rap1. Human cells contain a candidate overhang-binding protein, POT1, which is related to Cdc13 and other oligosaccharide/oligonucleotide-binding (OB) fold proteins with single-stranded telomeric DNA-binding activity[17–20]. Our data suggest that interactions between POT1 and the TRF1 complex allow POT1 to transduce information about telomere length to the telomere terminus, where the regulation of telomerase takes place.

To study the association of POT1 and other proteins with telomeres, we developed a chromatin immunoprecipitation (ChIP) assay, in which protein-associated telomeric DNA is detected by quantitative hybridization of a TTAGGG repeat probe to DNA dot blots (Fig. 1a–c; see also Supplementary Fig. 1). Alu sequences are used as a negative control in each experiment (Fig. 1c). As a second negative control, ChIPs were performed with various pre-immune sera, which yielded background signals (Fig. 1a–c). By contrast, TRF1 ChIPs yielded about 30% (28 ± 4; $n = 7$) of the total telomeric DNA in the HT1080-derived cell line HTC75 (data not shown). Similar telomeric DNA yields were obtained in TRF1 ChIPs in a variety of cell strains, including GM847, HeLa, IMR90 and BJ cells (Fig. 1 and data not shown). As the ChIP values are presented as a percentage of the total telomeric DNA, they are

corrected for telomere length variations in different cell lines. The telomeric association of TRF1-interacting protein 2 (TIN2) and components of the TRF2 complex was also readily detectable by ChIP. The yield of telomeric DNA was approximately 15% for TRF2 and its interacting partner human RAP1 (Fig. 1), and 10–15% for TIN2 (see below). Two rabbit anti-peptide antibodies to POT1 as well as two sera raised against the full-length protein immunoprecipitated a significant fraction (about 10%) of the telomeric DNA in ChIPs from HTC75 and GM847 cells (Fig.1; see also Supplementary Fig.1). Consistent with this finding, two of these sera (1048 and 1049) also detected POT1 at telomeres by immunofluorescence (Supplementary Fig. 1). Furthermore, telomeric DNA was recovered in ChIPs with a Myc antibody in cells expressing Myc–POT1 (Fig. 1a). Thus, POT1 behaves as a telomeric protein on the basis of ChIP and immunofluorescence.

As POT1 binds to single-stranded telomeric TTAGGG repeats but not to duplex telomeric DNA *in vitro*[17,18] (D.L., H. Parsons, K. Hoke and T.d.L., unpublished data), we anticipated that the telomeric binding of POT1 requires the presence of the 3′ telomeric overhang. To test this mode of binding *in vivo*, we made use of the fact that inhibition of the telomere protective factor TRF2 results in loss of 50% of the single-stranded telomeric DNA but leaves the duplex part of the telomere intact[21]. TRF2 was inhibited using two doxycyclin-regulated cell lines (T4 and T19) that express the TRF2(ΔBΔM) dominant-negative allele of TRF2 (ref. 21). As expected, induction of TRF2(ΔBΔM) resulted in a significant reduction (twofold, $P = 0.027$) in the binding of TRF2 to telomeres as assessed by ChIP (Fig. 1b, c). Furthermore, there was an associated loss of the TRF2-interacting factor RAP1 from the telomeres (sixfold reduction, $P = 0.009$; Fig. 1b, c) and about 50% loss of the 3′ overhang (data not shown). The amount of POT1 at telomeres was also reduced at least twofold in cells expressing TRF2(ΔBΔM) compared with uninduced controls (Wilcoxon two-sample test, $P = 0.013$; Fig. 1b, c). As a control, TRF1 was not significantly affected by inhibition of TRF2 (Fig. 1b, c; see also ref. 21). Thus, the diminished POT1 binding to telomeres correlated with a reduction in the amount of single-stranded telomeric DNA. The lack of interaction with TRF2 and RAP1 (see below) argues against the possibility that TRF2(ΔBΔM) removed POT1 from telomeres through protein interaction. However, we cannot rule out an indirect effect of the perturbation of the whole telomeric structure on POT1 binding.

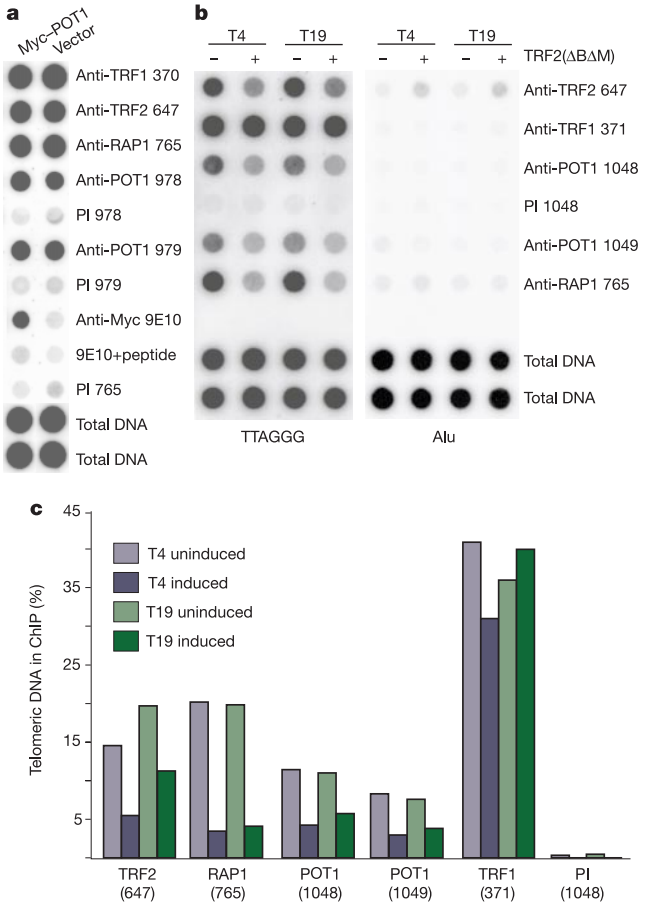

Figure 1 Telomeric association of POT1 correlates with single-stranded DNA (ssDNA). **a**, Telomeric ChIP on GM847 cells infected with pLPC or pLPC–Myc–POT1 using the indicated antibodies or pre-immune serum (PI). Dot blots were hybridized with a TTAGGG repeat probe. **b**, ChIP after reduction in telomeric overhang DNA owing to inhibition of TRF2. HTC75 clones T4 and T19 were induced (+) to express TRF2(ΔBΔM) for 7 days and were processed alongside uninduced cells (−). Duplicate dot blots were probed for telomeric or Alu repeats. **c**, Quantification of the data in **b** representing per cent TTAGGG repeat DNA recovered in each ChIP. Averaged duplicate signals obtained with total DNA samples were used as 100% value for the quantification.

Biochemical studies showed that the amino-terminal OB fold of POT1 is required for DNA binding[17,18] (D.L., H. Parsons, K. Hoke, J. Donigian and T.d.L., unpublished data). To test the role of the POT1 OB fold in telomere binding, we examined the localization of a mutant lacking the N-terminal 127 amino acids (POT1(ΔOB); Fig. 2a). Myc-tagged full-length POT1 and POT1(ΔOB) yielded proteins of the predicted molecular mass detectable with anti-Myc sera as well as with two antibodies raised against a POT1 peptide (Fig. 2b). Although the anti-peptide antibodies should detect four of the five proposed splice variants of POT1 (ref. 18), only a single endogenous protein was detected by both sera in HTC75 and HeLa cells and this polypeptide had an apparent molecular mass consistent with full-length POT1 (Fig. 2b and data not shown). Moderate overexpression of exogenous Myc–POT1 and Myc–POT1(ΔOB) resulted in nearly complete suppression of endogenous POT1 protein detectable by immunoblotting (Fig. 2b); the mechanism of this downregulation is not known. Immunofluorescence showed that POT1(ΔOB) still had the ability to localize to telomeres (Fig. 2c). This result was unexpected as we anticipated the DNA-binding domain of POT1 to be required for targeting to telomeres. We confirmed the telomeric association of POT1(ΔOB) using the ChIP assay (Fig. 2d, e). In these experiments, ChIPs with POT1 antibodies using cells expressing Myc–POT1(ΔOB) or Myc-tagged full-length POT1 resulted in the same yield of approximately 7% of the telomeric DNA. ChIPs with the Myc antibody were less efficient, but still yielded a significant fraction of telomeric DNA (about 2.5%) even when Myc-tagged POT1 lacked the OB fold (Fig. 2d, e). Although variations in expression levels interfere with direct comparison between the telomeric association of POT1(ΔOB) and full-length POT1, the data indicate that POT1(ΔOB) can still locate to telomeres. Owing to the very low abundance of endogenous POT1 in cells expressing POT1(ΔOB), it is unlikely that the telomeric association of POT1(ΔOB) occurs through an interaction with the endogenous full-length protein. Hence, the telomere localization of POT1(ΔOB) suggested that direct DNA binding mediated by the N-terminal OB fold is not the only mode of recruitment of POT1 to telomeres.

Therefore, we explored the possibility that POT1 interacts with the telomeric protein complexes formed by TRF1 and TRF2. Co-immunoprecipitation experiments showed that TRF1 associated with Myc-tagged POT1 (Fig. 3a), and immunoprecipitation of endogenous POT1 resulted in recovery of the TRF1-interacting factors TIN2 and tankyrase 1 (Fig. 3b–d). In parallel experiments, no interaction was detected between POT1 and TRF2 or its interacting partners RAP1 or Mre11 (refs 22, 23) (Fig. 3a, b; see also Supplementary Fig. 2), indicating that the association of POT1 with the TRF1 complex was highly specific. The association of POT1 with

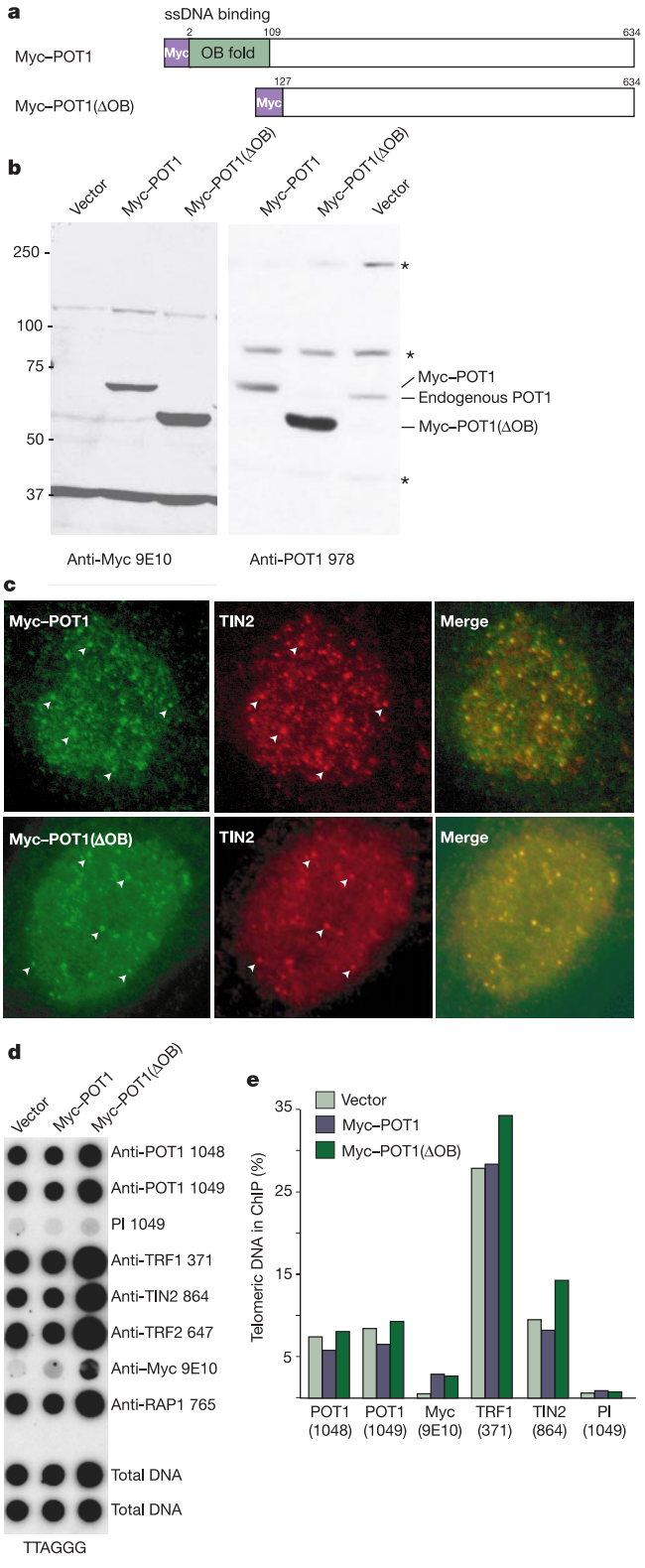

Figure 2 Telomeric association of POT1(ΔOB). **a**, POT1(ΔOB). **b**, Immunoblot of HTC75 cells infected with Myc–POT1, Myc–POT1(ΔOB) or pLPC probed for Myc or POT1. Asterisks indicate nonspecific bands (not detected by duplicate POT1 serum 979). Molecular mass standards (kDa) are shown on the left-hand side. **c**, Myc (9E10) and TIN2 (864) immuno fluorescence of IMR90 cells expressing Myc–POT1 or Myc–POT1(ΔOB). Arrowheads indicate examples of POT1 localizing together with TIN2. Both POT1 forms show non-telomeric signals. **d**, ChIPs on HTC75 cells containing the indicated retroviruses. Owing to telomere elongation over 150 population doublings, the TTAGGG signals are 3.5-fold higher for Myc–POT1(ΔOB). **e**, Quantification of the data in **d** (as in Fig. 1c). As the histograms represent the percentage of input telomeric DNA, they are corrected for telomere length changes.

the TRF1 complex was not dependent on the OB fold, as Myc-tagged POT1(ΔOB) was recovered in association with both TRF1 and TIN2 (Fig. 3a, b). Thus, the binding of POT1(ΔOB) to telomeres could be explained by the interaction of POT1 with the TRF1 complex.

To test whether the accumulation of POT1 on telomeres depended on its interaction with the TRF1 complex, we used tankyrase 1 overexpression, which is the most effective method for removing the TRF1 complex from telomeres[7]. Poly(ADP-ribosyl)ation of TRF1 by the PARP activity of tankyrase 1 results in loss of its DNA-binding activity *in vitro*[24], and this effect is thought to be

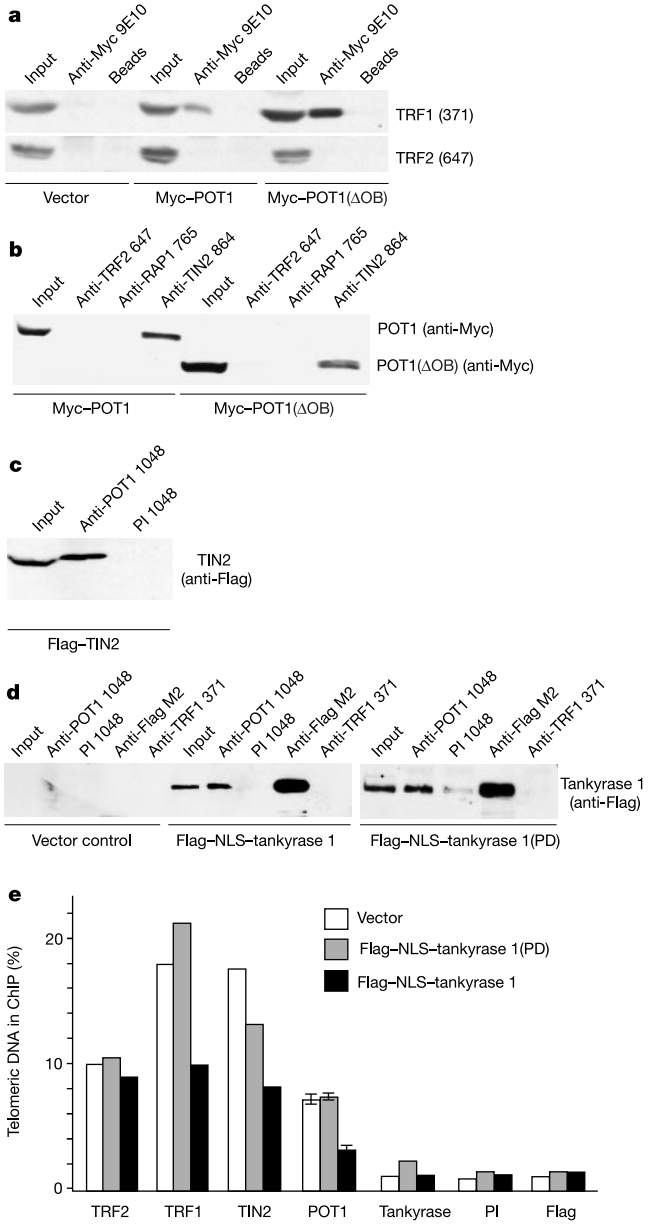

Figure 3 POT1 binds the TRF1 complex and is affected by tankyrase 1. **a**–**d**, Co-immunoprecipitation of POT1 and POT1(ΔOB) with TRF1, TIN2 and tankyrase 1 from HTC75 cells infected with the indicated retroviruses. Immunoprecipitated antibodies are indicated above the lanes. Input, 12% of input extract; PI, pre-immune serum; beads, BSA-blocked beads. Immunoblot antibodies are indicated on the right. **e**, ChIP on HTC75 cells infected with Flag–NLS–tankyrase 1, Flag–NLS–tankyrase 1(PD) or the pLPC vector (as in Fig. 1). POT1 values represent median and standard deviations ($n = 4$). For dot blots see Supplementary Fig. 1.

responsible for the loss of the TRF1 complex from telomeres in cells overexpressing tankyrase 1 in the nucleus[7]. As a control, we used cells expressing the same level of a mutated PARP-dead derivative of tankyrase 1 (tankyrase 1(PD)) that does not remove TRF1 from telomeres (J. Ye and T.d.L., manuscript in preparation; see also ref. 25). As previously observed by immunofluorescence[7], ChIP data indicated that overexpression of catalytically active tankyrase 1 resulted in diminished telomeric association of TRF1 and TIN2 (Fig. 3e; see also Supplementary Fig. 3). We found that overexpression of tankyrase 1, but not the PARP-dead derivative, reduced by half the amount of POT1 on telomeres as determined by ChIP (twofold reduction, $P = 0.009$; Fig. 3e; see also Supplementary Fig. 3). We note that POT1 is able to interact with both PARP-dead and active tankyrase 1 (Fig. 3d), suggesting that the effect seen with wild-type tankyrase 1 is not simply due to titration by overexpression. TRF2, which serves as a negative control, was not affected by tankyrase 1 (Fig. 3e). Furthermore, the telomeric overhangs were not altered in the cell lines expressing tankyrase 1 or its PARP-dead derivative (Supplementary Fig. 3). Taken together, these data suggest that POT1 is recruited to telomeres through an interaction with the TRF1 complex.

Because the TRF1 complex regulates telomere length, we tested whether POT1 could also affect the steady-state length of human telomeres. Expression of POT1(ΔOB) induced exceptionally rapid telomere elongation (about 230 base pairs per end per population doubling) in HTC75 cells whereas vector control cells maintained stable telomeres (Fig. 4a, b). This rate of telomere elongation exceeds the growth rate of newly formed telomeres[11] and is also faster than the rate of telomere elongation observed in experiments that altered TRF1-mediated length control[5,7,8]. The POT1(ΔOB) telomeres continued to elongate over at least 150 population doublings, resulting in ultra-long telomeres detectable in genomic blots and in a commensurate increase in TTAGGG repeat signal in dot blots (Fig. 2d). Myc-tagged full-length POT1 did not affect telomere length (Fig. 4b). Neither form of POT1 affected the G-strand overhang signal in HTC75 cells as determined by in-gel analysis (data not shown). The telomere elongation phenotype of POT1(ΔOB) is not attributable to changes in the amount of TRF1 or TIN2 on the telomeres, as ChIP experiments showed that POT1(ΔOB) did not decrease the presence of these proteins (Fig. 2d, e). The finding that these telomeres contained normal amounts of TRF1, yet elongated at a very high rate, indicates that POT1(ΔOB) abrogated the TRF1-mediated inhibition of telomere elongation. This is consistent with POT1 being a downstream effector of the TRF1 pathway and POT1(ΔOB) being defective in this function.

According to the protein-counting model for telomere length homeostasis, longer telomeres should contain larger amounts of the TRF1 complex. We used ChIP of cells with long and short telomeres to test this. HeLa1.2.11 cells have exceptionally long telomeres of

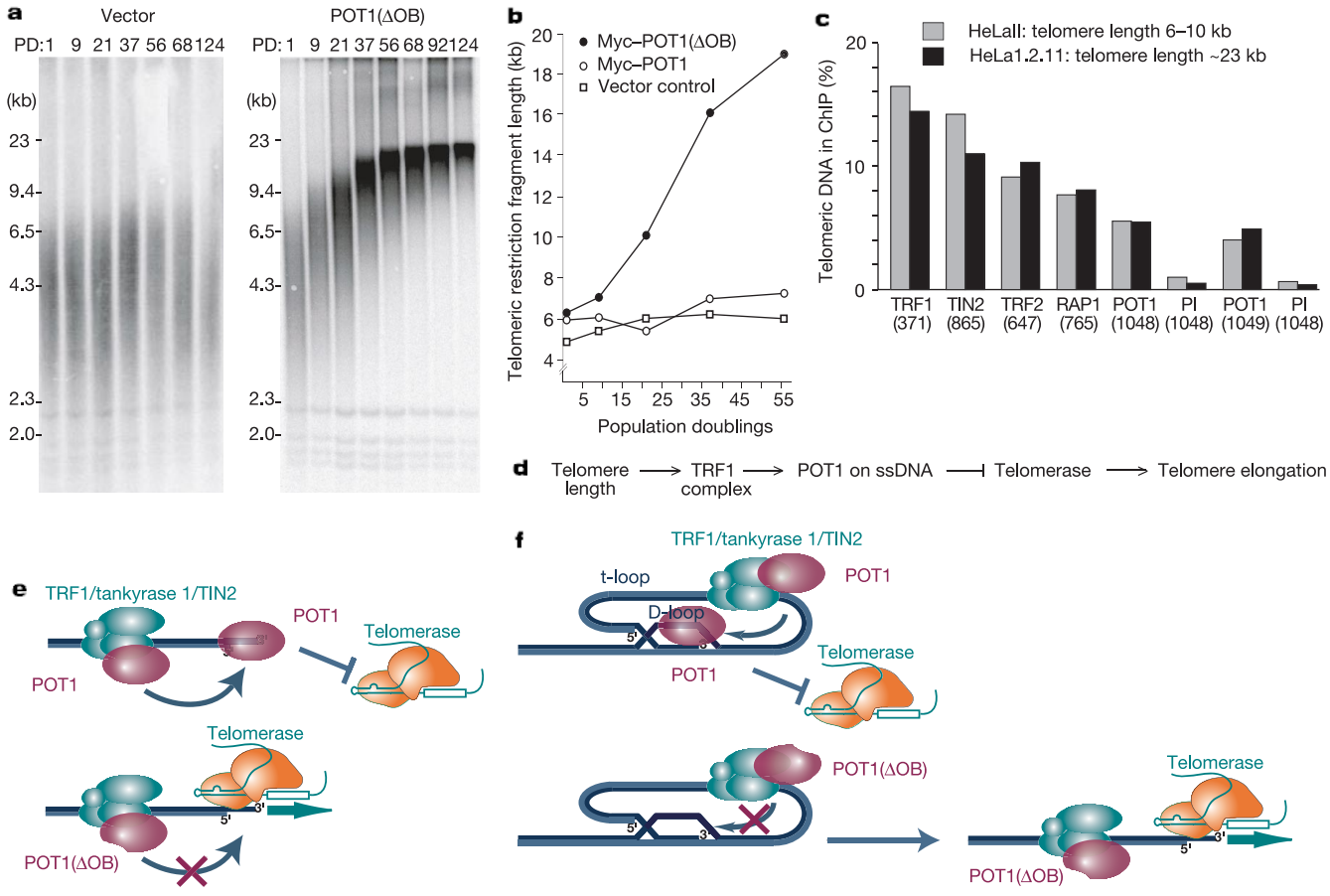

Figure 4 POT1 regulates telomere length. **a**, Genomic blots of telomeric restriction fragments in HTC75 cells at the indicated population doubling (PD) expressing Myc–POT1(ΔOB) or no exogenous protein. **b**, Median telomeric fragment lengths in the indicated cell lines plotted against population doubling. **c**, ChIP yields on telomeres of HeLa1.2.11 and HeLaII cells. ChIP values are corrected for telomere length as in Fig. 1. As telomeres of HeLa1.2.11 cells are threefold longer than telomeres of HeLaII cells, equivalent ChIP of the telomeric DNA in both cell lines indicates that the HeLa1.2.11 ChIP brought down threefold more telomeric DNA. For dot blots see Supplementary Fig. 4b. **d**–**f**, Models proposing a role for POT1 as a terminal transducer of TRF1 telomere length control. See text for discussion.

approximately 23 kilobases (kb) in length, whereas another HeLa subclone, HeLaII, has canonical telomeres in the range of 6–10 kb (ref. 26). In agreement, dot blots indicated that HeLa1.2.11 had about 2.9-fold higher relative abundance of telomeric sequences (Supplementary Fig. 4a). The telomeres in the two HeLa subclones only differ in the length of the duplex telomeric repeat array (Supplementary Fig. 4c)[26]; the 3′ telomeric overhangs in the two HeLa cell lines are similar (Supplementary Fig. 4c, d). Comparison of ChIPs with antibodies to TRF1 and TIN2 revealed that the fraction of precipitated telomeric DNA in the two HeLa lines was independent of telomere length (Fig. 4c; see also Supplementary Fig. 4b). Thus, the same fraction of telomeric DNA (about 15%) was recovered in TRF1 ChIPs in the two HeLa cell lines. This result is consistent with previous immunofluorescence data[6] and indicates that longer telomeres contain a higher number of TRF1 complexes. Similarly, the fraction of precipitated telomeric DNA in TRF1 ChIPs was independent of telomere length in two HTC75 cell lines that differed in telomere length by a factor of 3.5 owing to expression of POT1(ΔOB) (Fig. 2d, e). The POT1 ChIP efficiency was also the same in HeLaII and HeLa1.2.11 cell lines (Fig. 4c), suggesting that long telomeres recruited more POT1 than short telomeres. We note that the increased association of POT1 with longer telomeres could be due to more efficient loading of POT1 on single-stranded TTAGGG repeats, or to recruitment along the duplex part of the telomere by protein interaction. The ChIP technique cannot differentiate between these two possibilities owing to the lack of specificity in the crosslinking.

These data demonstrate that the human single-stranded telomeric DNA-binding protein POT1 responds to the telomere length regulatory pathway governed by the TRF1 complex (Fig. 4d). The TRF1 complex binds along the duplex part of the telomere and functions as a measuring device to assess telomere length. For telomere length homeostasis to be effective, information about the length of the telomere needs to be relayed from the TRF1 complex to the single-stranded part of the telomere where telomerase is regulated. Our data indicate that POT1 transduces this information (Fig. 4d–f). The two critical features of POT1 that allow it to relay information about telomere length to the telomere terminus are that it binds to single-stranded telomeric DNA and that its accumulation on telomeres is, in part, regulated by the TRF1 complex.

We predict two possible ways in which POT1 might act to relay telomere length information to telomerase (Fig. 4e, f). The TRF1 complex might recruit POT1 to the telomeric chromatin and facilitate its accumulation on the single-stranded DNA at the nearby telomere terminus. Once located on the single-stranded DNA, POT1, which has a slight preference for 3′ ends[27] (D.L., H. Parsons, K. Hoke and T.d.L., unpublished data), might sequester the telomere terminus and thus directly block telomerase from elongating the telomeric DNA (Fig. 4e). Alternatively, the recruitment of POT1 to the telomeric chromatin could facilitate its binding to the single-stranded DNA (D-loop) at the base of the t-loop (Fig. 4f). Biochemical studies indicate that POT1 has the ability to bind to single-stranded telomeric DNA in the absence of a 3′ end (D.L., H. Parsons, K. Hoke and T.d.L., unpublished data). The binding of POT1 to the D-loop could stabilize telomeres in the t-loop configuration and thus inhibit telomerase by indirect sequestration of the 3′ terminus. Both models predict that the POT1(ΔOB) mutant, which lacks the single-stranded DNA-binding activity, will fail to inhibit telomerase, even though POT1(ΔOB) is recruited to the telomeric chromatin by the TRF1 complex (Fig. 4e, f). Thus, POT1(ΔOB) expression will abrogate TRF1-mediated telomere length control, resulting in the observed extensive telomere elongation phenotype. In both versions of the model, control of telomere length is achieved when the larger mass of TRF1 on longer telomeres leads to increased loading of POT1 on the single-stranded telomeric DNA. Depending on the loading of POT1 on the single-stranded DNA, the probability that telomerase becomes inhibited at the telomere terminus will be increased. □

Methods

POT1 constructs, cell lines and antibodies

A full-length human POT1 complementary DNA (Supplementary Information) was generated by polymerase chain reaction (PCR) and cloned into FastBac and into the pLPC retroviral vector with a Myc epitope tag replacing the start codon. POT1(ΔOB) was constructed by PCR and represents amino acids 127–634 preceded by the Myc epitope tag. GM847 cells were obtained from the American Type Culture Collection. Myc-tagged POT1 and POT1(ΔOB) were retrovirally expressed in HTC75 cells as described[28]. HTC75 cells infected with retroviruses expressing Flag–NLS–tankyrase 1 and Flag–NLS–tankyrase 1(PD) were provided by J. Ye (J. Ye and T.d.L., manuscript in preparation). All cell lines were grown in DMEM, 15% fetal bovine serum with appropriate antibiotics as described[21,28]. Antibodies 978 and 979 were affinity purified from rabbit serum to a keyhole limpet haemocyanin-conjugated POT1 peptide (CYGRGIRVLPESNSDVDQLKKDLES representing amino acids 271–294 plus a Cys residue). Antibodies 1048 and 1049 were affinity purified from rabbit serum raised against baculovirus-derived POT1. The TIN2 antibody 864 will be described elsewhere (J. Ye and T.d.L., manuscript in preparation). Antibodies to TRF1, TRF2, RAP1 and the Mre11 complex have been described[5,6,22,23]. 9E10 antibody to the Myc epitope was from Oncogene Biosciences and the M2 Flag antibody was from Sigma.

Chromatin immunoprecipitations

For ChIPs, cells were digested with trypsin, washed with PBS, fixed in 1% formaldehyde in PBS for 60 min at room temperature, washed with PBS, and lysed in 1% SDS, 50 mM Tris-HCl, pH 8.0, 10 mM EDTA at a density of 10^7 cells ml^{-1}. Lysates were sonicated to obtain chromatin fragments <1 kb, and centrifuged for 10 min in a microfuge at 4 °C. Two hundred microlitres of lysate, diluted with 1.2 ml 0.01% SDS, 1.1% Triton X-100, 1.2 mM EDTA, 16.7 mM Tris-HCl, pH 8.0, and 150 mM NaCl was supplemented with antibody (typically 20 μl crude serum or 5 μl 9E10), mutated overnight at 4 °C, supplemented with 30 μl protein G Sepharose beads (Amersham; blocked with 30 μg bovine serum albumin (BSA) and 5 μg sheared *Escherichia coli* DNA), and incubated for 30 min at 4 °C. Immunoprecipitated pellets were washed with 0.1% SDS, 1% Triton X-100, 2 mM EDTA, pH 8.0, 20 mM Tris-HCl, pH 8.0, containing 150 mM NaCl in the first wash and 500 mM NaCl in the second wash. Further washes were with 0.25 M LiCl, 1% NP-40, 1% Na-deoxycholate, 1 mM EDTA, pH 8.0, 10 mM Tris-HCl, pH 8.0, and with 10 mM Tris-HCl, pH 8.0, 1 mM EDTA. Chromatin was eluted from the beads with 500 μl 1% SDS, 0.1 M Na_2CO_3. After addition of 20 μl of 5 M NaCl, crosslinks were reversed for 4 h at 65 °C. Samples were supplemented with 20 μl of 1 M Tris-HCl, pH 6.5, 10 μl of 0.5 M EDTA, and 20 μg DNase free RNase A, and incubated at 37 °C for 30 min. Samples were then digested with 40 μg proteinase K for 60 min at 37 °C, phenol extracted, and the DNA was precipitated overnight at −20 °C with 1 ml ethanol. The precipitate was dissolved in 100 μl water, denatured at 95 °C for 5 min, and dot blotted onto Hybond membranes in 2 × SSC (80% was loaded for the detection of telomeric sequences, and 10% for Alu sequences). Membranes were treated with 1.5 M NaCl, 0.5 N NaOH for 10 min, and with 1 M NaCl, 0.5 M Tris-HCl, pH 7.0, for 10 min. Hybridization with a 800-bp Klenow-labelled TTAGGG probe or an Alu probe was performed as described previously[29]; membranes were washed four times in 2 × SSC and exposed overnight to PhosphorImager screen. The quantification of the per cent precipitated DNA was done with the ImageQuant software. All lysates were normalized for cell number. For the total telomeric DNA samples, two 50-μl aliquots (corresponding to one-quarter of the amount of lysate used in the immunoprecipitations) were processed along with the rest of the samples at the step of reversing the crosslinks. The average of the telomeric signal in two total fractions was taken for the reference value (total DNA), and the percentage of each immunoprecipitation sample was calculated based on the signal relative to the corresponding total DNA signal. Therefore, the calculated ChIP yield takes into account changes in telomere length. Initial control experiments were done to ensure that the amount of antibody and duration of crosslinking were not limiting in the ChIP yields.

Telomere assays and other analyses

Telomere length and overhang assays were as described[28]. Immunoprecipitations and immunoblotting were performed using standard protocols (Supplementary Information) except for the detection of POT1, which involved guanidine re-naturation (see Supplementary Information for details). Immunofluorescence was performed using previously published procedures[5] (see Supplementary Information for details).

Received 26 February; accepted 29 April 2003; doi:10.1038/nature01688.
Published online 25 May 2003.

1. Blackburn, E. H. Telomere states and cell fates. *Nature* **408,** 53–56 (2000).
2. de Lange, T. Protection of mammalian telomeres. *Oncogene* **21,** 532–540 (2002).
3. Granger, M. P., Wright, W. E. & Shay, J. W. Telomerase in cancer and aging. *Crit. Rev. Oncol. Hematol.* **41,** 29–40 (2002).
4. Maser, R. S. & DePinho, R. A. Connecting chromosomes, crisis, and cancer. *Science* **297,** 565–569 (2002).
5. van Steensel, B. & de Lange, T. Control of telomere length by the human telomeric protein TRF1. *Nature* **385,** 740–743 (1997).
6. Smogorzewska, A. *et al.* Control of human telomere length by TRF1 and TRF2. *Mol. Cell. Biol.* **20,** 1659–1668 (2000).
7. Smith, S. & de Lange, T. Tankyrase promotes telomere elongation in human cells. *Curr. Biol.* **10,** 1299–1302 (2000).

8. Kim, S. H., Kaminker, P. & Campisi, J. TIN2, a new regulator of telomere length in human cells. *Nature Genet.* **23,** 405–412 (1999).
9. Zhou, X. Z. & Lu, K. P. The Pin2/TRF1-interacting protein PinX1 is a potent telomerase inhibitor. *Cell* **107,** 347–359 (2001).
10. Ancelin, K. *et al.* Targeting assay to study the *cis* functions of human telomeric proteins: evidence for inhibition of telomerase by TRF1 and for activation of telomere degradation by TRF2. *Mol. Cell. Biol.* **22,** 3474–3487 (2002).
11. Barnett, M. A. *et al.* Telomere directed fragmentation of mammalian chromosomes. *Nucleic Acids Res.* **21,** 27–36 (1993).
12. Hanish, J. P., Yanowitz, J. L. & de Lange, T. Stringent sequence requirements for the formation of human telomeres. *Proc. Natl Acad. Sci. USA* **91,** 8861–8865 (1994).
13. Sprung, C. N., Reynolds, G. E., Jasin, M. & Murnane, J. P. Chromosome healing in mouse embryonic stem cells. *Proc. Natl Acad. Sci. USA* **96,** 6781–6786 (1999).
14. Sprung, C. N., Sabatier, L. & Murnane, J. P. Telomere dynamics in a human cancer cell line. *Exp. Cell Res.* **247,** 29–37 (1999).
15. Marcand, S., Gilson, E. & Shore, D. A protein-counting mechanism for telomere length regulation in yeast. *Science* **275,** 986–990 (1997).
16. Evans, S. K. & Lundblad, V. Positive and negative regulation of telomerase access to the telomere. *J. Cell Sci.* **113,** 3357–3364 (2000).
17. Baumann, P. & Cech, T. R. Pot1, the putative telomere end-binding protein in fission yeast and humans. *Science* **292,** 1171–1175 (2001).
18. Baumann, P., Podell, E. & Cech, T. R. Human Pot1 (protection of telomeres) protein: cytolocalization, gene structure, and alternative splicing. *Mol. Cell. Biol.* **22,** 8079–8087 (2002).
19. de Lange, T. Telomere capping—one strand fits all. *Science* **292,** 1075–1076 (2001).
20. Mitton-Fry, R. M., Anderson, E. M., Hughes, T. R., Lundblad, V. & Wuttke, D. S. Conserved structure for single-stranded telomeric DNA recognition. *Science* **296,** 145–147 (2002).
21. van Steensel, B., Smogorzewska, A. & de Lange, T. TRF2 protects human telomeres from end-to-end fusions. *Cell* **92,** 401–413 (1998).
22. Li, B., Oestreich, S. & de Lange, T. Identification of human Rap1: implications for telomere evolution. *Cell* **101,** 471–483 (2000).
23. Zhu, X. D., Kuster, B., Mann, M., Petrini, J. H. & Lange, T. Cell-cycle-regulated association of RAD50/MRE11/NBS1 with TRF2 and human telomeres. *Nature Genet.* **25,** 347–352 (2000).
24. Smith, S., Giriat, I., Schmitt, A. & de Lange, T. Tankyrase, a poly(ADP-ribose) polymerase at human telomeres. *Science* **282,** 1484–1487 (1998).
25. Cook, B. D., Dynek, J. N., Chang, W., Shostak, G. & Smith, S. Role for the related poly(ADP-Ribose) polymerases tankyrase 1 and 2 at human telomeres. *Mol. Cell. Biol.* **22,** 332–342 (2002).
26. Griffith, J. D. *et al.* Mammalian telomeres end in a large duplex loop. *Cell* **97,** 503–514 (1999).
27. Lei, M., Baumann, P. & Cech, T. R. Cooperative binding of single-stranded telomeric DNA by the Pot1 protein of *Schizosaccharomyces pombe*. *Biochemistry* **41,** 14560–14568 (2002).
28. Karlseder, J., Smogorzewska, A. & de Lange, T. Senescence induced by altered telomere state, not telomere loss. *Science* **295,** 2446–2449 (2002).
29. de Lange, T. *et al.* Structure and variability of human chromosome ends. *Mol. Cell. Biol.* **10,** 518–527 (1990).

Supplementary Information accompanies the paper on **www.nature.com/nature**.

Acknowledgements We are grateful to J. Ye for providing numerous critical reagents for these studies. H. Parsons provided excellent technical assistance. Members of the de Lange laboratory are thanked for comments on this work. This work was supported by a grant from the NIH. D.L. is a recipient of an Ann Siegel Postdoctoral fellowship from the ACS.

Competing interests statement The authors declare that they have no competing financial interests.

Correspondence and requests for materials should be addressed to T.d.L. (delange@mail.rockefeller.edu).

corrigendum

Selection of evolutionarily conserved mucosal-associated invariant T cells by MR1

Emmanuel Treiner, Livine Duban, Seiamak Bahram, Mirjana Radosavljevic, Valerie Wanner, Florence Tilloy, Pierre Affaticati, Susan Gilfillan & Olivier Lantz

Nature **422**, 164–169 (2003).

Owing to mislabelling by the mouse provider, the strain of mice used as a control in the experiment shown in Fig. 4 was not C3H/HeJ but C3H/HeOu. C3H/HeJ have a defect in TLR4-mediated signalling that the other C3H strains do not have. This correction does not affect our conclusions. □

addendum

Non-classical receptive field mediates switch in a sensory neuron's frequency tuning

Maurice J. Chacron, Brent Doiron, Leonard Maler, André Longtin & Joseph Bastian

Nature **423**, 77–81 (2003).

In this Letter, we inadvertently omitted to give the species name, *Apteronotus leptorhynchus* (brown ghost knife-fish), of the weakly electric fish used in our study. □

Supplemental Material

Methods

Cloning of hPot1

A full length human Pot1 cDNA was generated by PCR. Most of the ORF was derived from a Pot1 EST from the ATCC (#aa66f08.s1), encoding an N-terminally truncated protein; the N-terminus from the start codon to the NdeI site at bp 427 was obtained by reverse transcription of HeLa RNA. The resulting cDNA was identical to the published cDNA [18] and to GenBank entry # FLJ11073.

Protein extracts, co-immunoprecipitations, and Western blot

Cells were trypsinized, washed once with culture medium and once with PBS, and lysed in 0.5 ml lysis buffer (50 mM Tris-HCl pH 7.4/1% Triton X-100/ 0.1% SDS/150 mM NaCl/1 mM EDTA/1 mM DTT/1mM PMSF, 1 µg aprotinin per ml, 10 µg pepstatin per ml, 1 µg leupeptin per ml). Nuclear proteins were extracted by adding 25 µl of 5 M NaCl and incubating on ice for 20 min. Lysates were diluted with 0.5 ml of cold water and centrifuged in a microfuge at 4^{o}C for 10 min at maximum speed. Supernatants (200 µl/IP) were immuno-precipitated for 4 hr at 4^{o}C with 20 µl of rabbit serum, 5 µl of 9E10, or 2µl of M2. Immune complexes were bound for 30 min at 4^{o}C to 30 µl of Protein G Sepharose beads blocked with BSA. The beads were washed twice with lysis buffer and resuspended in 50 µl of Laemmli buffer (50 mM Tris-HCl pH 6.8/4% SDS/20% Glycerol/5% β-mercaptoethanol/0.01% Bromophenol Blue) and 20 µl was fractionated on SDS-PAGE gels alongside total fractions. Western blotting and membrane incubations were performed as described previously[30]. Blots with the 978 anti-peptide antibody to detect hPot1 were performed as follows. After transfer onto nitrocellulose, the membrane was incubated in decreasing concentrations of guanidine (6 M, 3 M, 1 M, 0.1 M) in AC buffer (10% glycerol/100 mM NaCl/20 mM Tris-HCl pH 7.5/1 mM EDTA/0.1% Tween 20/2% non-fat dry milk powder/1 mM DTT). All incubations were performed at rt for 30 min. The membrane was then incubated overnight in AC buffer without Guanidine, washed with PBS/0.1% Tween 20 and subjected to conventional primary and secondary incubations. The affinity purified 978 antibody was used at a dilution of 1:1000, the 9E10 at 1:1000, and the M2 anti-FLAG at 1:10,000.

Immunofluorescence

Cells were grown on coverslips, washed with PBS, fixed in 2% paraformaldehyde (Sigma P-6148) for 10 min and permeabilized in PBS/0.5% NP40 for 10 min. The coverslips were washed twice with PBS and blocked with PBG (0.2% (w/v) cold water fish gelatin (Sigma G-7765), 0.5% (w/v) BSA (Sigma A-2153) in PBS) for 40 min. Primary antibody incubations were performed at rt for 4 hr (1:2000 for Ab 1048 (hPot1), Ab 1049 (hPot1), Ab 864 (TIN2) and Ab 647 (TRF2); 1:1000 for 9E10 (myc) antibody). The coverslips were washed 3 times with PBG and incubated with the secondary antibody for 40 min at room temperature (Jackson Labs Donkey anti-Rabbit-TRITC or Donkey anti-Mouse-FITC, diluted 1:250). After 3 washes with PBG and one wash with PBS, cells were stained with DAPI (100 ng/ml) for 3 min, washed again with PBS and mounted on slides with 1mg/ml p-phenylene diamine (Sigma P-6001) in PBS/glycerol. Images were captured with an Axioplan 2 Zeiss microscope equipped with a Hamamatsu digital camera supported by OpenLab software.

Figures and Legends:

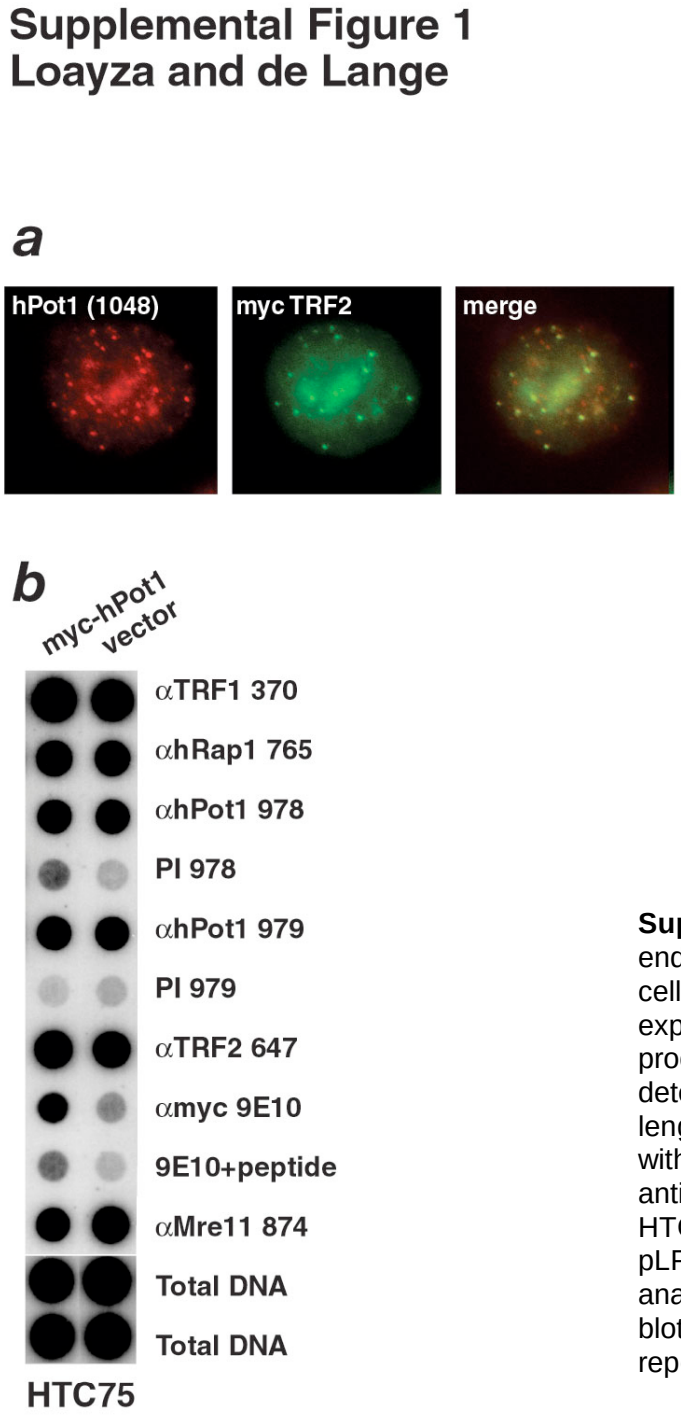

Supplemental Fig. 1. *a*, Co-localization of endogenous hPot1 with TRF2. HeLa1.2.11 cells were infected with a retrovirus expressing myc-tagged TRF2 and processed for IF. Endogenous hPot1 was detected with a rabbit serum against full length hPot1 (#1048, red) and co-localized with myc-TRF2 detected with the 9E10 antibody (green). **b,** Telomeric ChIP on HTC75 cells. Cells infected with pLPC or pLPC-myc-hPot1 were processed for ChIP analysis with the indicated antibodies. Dot-blots were hybridized with a TTAGGG repeat probe.

Supplemental Figure 2
Loayza and de Lange

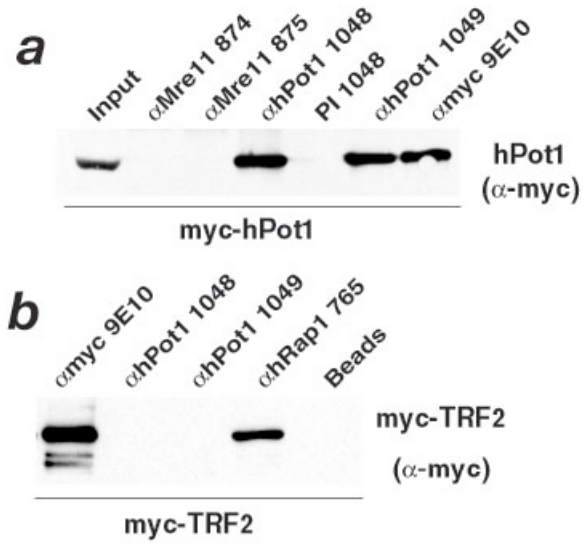

Supplemental Fig. 2. *a*, Specificity test for hPot1 sera 1048 and 1049 and lack of co-IP of Mre11 and hPot1. IPs from HTC75 cells expressing myc-hPot1 with the indicated antibodies, probed with the 9E10 myc tag antibody as indicated. ***b*,** Lack of co-IP of myc-tagged TRF2 with endogenous hPot1. IPs from HeLa 1.2.11 cells expressing myc-TRF2 using the indicated sera, probed with the 9E10 antibody. The hRap1 IP is a positive control for the detection of protein interaction with TRF2.

Supplemental Figure 3
Loayza and de Lange

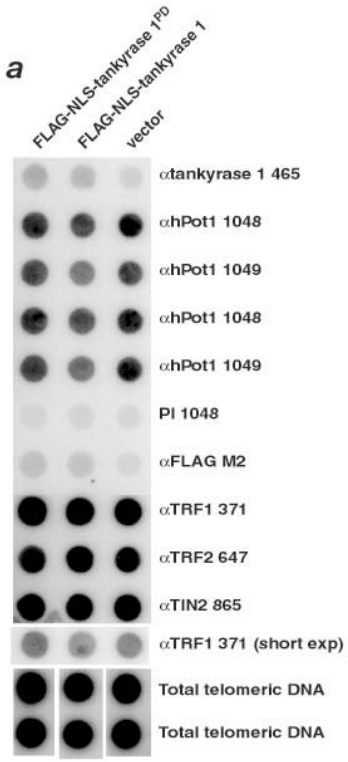

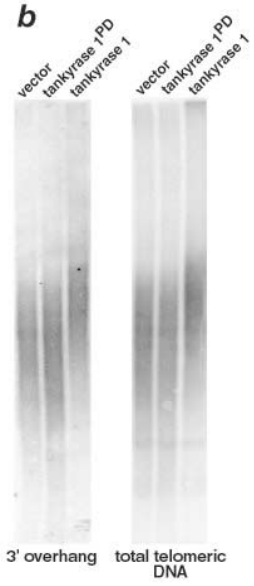

c

Cells/retrovirus	3' overhang signal (AU)	total tel. DNA signal (AU)	ratio
HTC75/vector	283	125	2.3
HTC75/tankyrase 1^{PD}	369	113	3.3
HTC75/tankyrase 1	367	130	2.8

Supplemental Fig. 3 ***a***, ChIP analysis of telomeric association of the indicated components in HTC75 cells expressing FLAG-NLS-tankyrase 1, FLAG-NLS-tankyrase 1^{PD}, or no exogenous protein (vector). For histogram, see Fig. 3e. ***b,*** Analysis of the telomeric overhangs by in-gel hybridization in HTC75 cells infected with the retroviral vector control (vector) or retroviruses expressing FLAG-NLS-tankyrase 1 or FLAG-NLS-tankyrase 1^{PD} (used in Fig.3e and panel a). Hybridization with a C-strand telomeric probe to native DNA detecting telomeric overhangs (left). Hybridization with the complementary strand did not reveal any signal (not shown). Right panel shows the total telomeric DNA in the same gel re-hybridized with the same probe after denaturation. Note that the telomeres in the tankyrase 1 expressing cells have elongated slightly. ***c***, Quantitation of the G-strand overhangs and total telomeric DNA signal of the panels shown in *b*, in arbitrary units. The ratio between the two values is a measure of the telomeric overhang signal.

Supplemental Figure 4
Loayza and de Lange

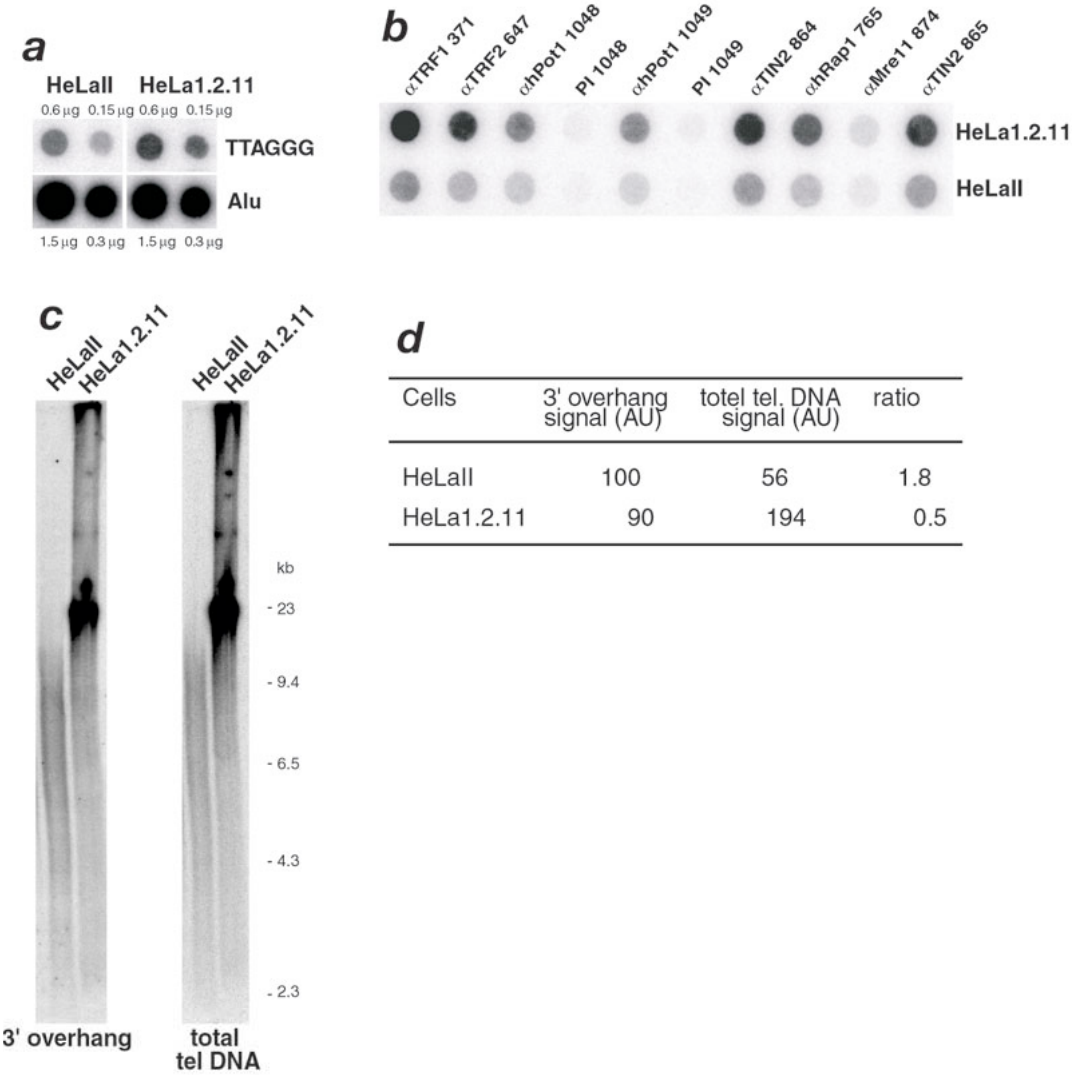

d

Cells	3' overhang signal (AU)	totel tel. DNA signal (AU)	ratio
HeLaII	100	56	1.8
HeLa1.2.11	90	194	0.5

Supplemental Fig. 4 a, Relative abundance of TTAGGG repeats in HeLa1.2.11 and HeLaII. Indicated amounts of total DNAs used for the ChIPs shown in Fig.4c and panel b were probed for TTAGGG (top row) or Alu sequences (bottom row). Quantitation of the signals indicates that HeLa1.2.11 has 3-fold more TTAGGG repeats than HeLaII, in good agreement with published telomere lengths determined by genomic blotting and EM analysis [26].***b*,** ChIP with the indicated antibodies in HeLa1.2.11 and HeLaII. Dot-blots were probed for TTAGGG repeats. For histogram, see Fig.4c.

c*,*d Measurement of the amount of telomeric overhangs in HeLa 1.2.11 versus HeLa II, as detected by in-gel hybridization. In gel hybridization and quantitation were performed as in Suppl. Fig.3b. The ratio between the two values (1.8 and 0.5) is accounted for by the difference in telomere length in these two cell lines and indicates that the telomeric overhangs are not significantly different.